Finite difference methods for orthorhombic media: perfectly reflecting and absorbing boundaries

P.F. Daley

ABSTRACT

An approach for the numerical solution of the forward problem for elastic wave propagation in a plane layered anisotropic (orthorhombic) elastic media is revisited. The introduction of an absorbing boundary at the model bottom is considered in this report. These boundary conditions are similar to those derived in Clayton and Engquist (1977). The stiffness coefficients (in Voigt notation), C_{ij} and the density, ρ, may vary arbitrarily with depth. The method discussed here employs finite Fourier transforms to temporarily remove the x and y coordinates resulting in a coupled system of three finite difference equations in the 3 Cartesian coordinate particle displacements in terms of depth (z) and time (t). The return to the (x, y, z, t) domain is done using a double inverse summation over the two horizontal wave numbers (k_x, k_y). The absorbing boundary conditions are only considered for the model bottom as there are alternate methods for the free surface and side boundaries. The full elastic equations are not used at the model bottom, but rather their scalar approximations. This may appear highly suspect, but reasonable results have been obtained for less complex media types and it was thought that it should at least be investigated for this case.

INTRODUCTION

In both theory and in numerical methods of solution of the forward problem difficulties arising are not to a large extent connected with a type of the given equations but to a larger extent with media dimension and the complexity of the properties of coefficients defining the media. Different physical effects when simulating elastic wave fields in seismology and seismic prospecting, which are not described by the acoustic wave equation, are obtained in this modeling procedure. Such effects should in reality be taken into account.

The finite difference method is a popular approach for solving elastic wave equations. However, in seismic problems where very large computation domains are considered, the use of the conventional numerical methods is limited by high computer costs and insufficient accuracy of these methods. This situation makes us focus on the development of an efficient numerical process which allows for the solution of $3D$ seismic problems.

This work describes a numerical algorithm for the forward seismic problem and has been presented in more detail in earlier reports. The main concept underlying the algorithm is the splitting of $3D$ problems to a series of coupled $1D$ problems in the (k_x, k_y, z, t) domain and their solution is then obtained sequentially using the finite

difference technique followed by finite inverse summations in the wave number domain, $\left(k_x, k_y\right)$

Depending on the behavior of coefficient variation, the algorithm may take on numerous forms. The version of the algorithm used here is based on a combination of finite Fourier integral transforms over the $\left(x, y\right)$ spatial coordinates with the finite difference techniques for solving the resulting $1D$ problems in the $\left(z, t\right)$ domain. The algorithm was suggested and developed in Mikhailenko (1985). Due to some typographic errors in that work, the relevant formulae required are once more given here.

In what follows, Lamb's problem for the anisotropic (orthorhombic) vertically inhomogeneous half-space with no dependence of the stiffness coefficients, C_{ij}, and density, ρ, on the horizontal $\left(x, y\right)$ coordinates. They may vary arbitrarily with depth $\left(z\right)$. Elastic wave propagation in such a medium is described by equations given in the next section.

THEORY

In a plane layered orthorhombic medium with no lateral inhomogeneities the particle displacement may be specified in a Cartesian coordinate system, $\left(x, y, z\right)$, as $\mathbf{u} = \left(u, v, w\right)$, where the vector components of displacement $\left(u, v, w\right)$ are the solutions of the coupled equations

$$\rho \frac{\partial^2 u}{\partial t^2} = C_{11} \frac{\partial^2 u}{\partial x^2} + C_{13} \frac{\partial^2 w}{\partial x \partial z} + C_{66} \frac{\partial^2 u}{\partial y^2} + \left(C_{12} + C_{66}\right) \frac{\partial^2 v}{\partial x \partial y} + \frac{\partial}{\partial z}\left(C_{55} \frac{\partial u}{\partial z}\right) + \frac{\partial}{\partial z}\left(C_{55} \frac{\partial w}{\partial x}\right) + F_x\left(x, y, z, t\right) \tag{1}$$

$$\rho \frac{\partial^2 v}{\partial t^2} = \left(C_{66} \frac{\partial^2 u}{\partial x \partial y} + C_{66} \frac{\partial^2 v}{\partial^2 x}\right) + C_{12} \frac{\partial^2 u}{\partial x \partial y} + C_{22} \frac{\partial^2 v}{\partial y^2} + C_{23} \frac{\partial^2 w}{\partial y \partial z} + \frac{\partial}{\partial z}\left(C_{44} \frac{\partial v}{\partial z}\right) + \frac{\partial}{\partial z}\left(C_{44} \frac{\partial w}{\partial y}\right) + F_y\left(x, y, z, t\right) \tag{2}$$

$$\rho\frac{\partial^2 w}{\partial t^2}=C_{55}\frac{\partial^2 u}{\partial x\partial z}+C_{55}\frac{\partial^2 w}{\partial x^2}+C_{44}\frac{\partial^2 v}{\partial y\partial z}+C_{44}\frac{\partial^2 w}{\partial y^2}+$$
$$\frac{\partial}{\partial z}\left(C_{13}\frac{\partial u}{\partial x}\right)+\frac{\partial}{\partial z}\left(C_{23}\frac{\partial v}{\partial y}\right)+\frac{\partial}{\partial z}\left(C_{33}\frac{\partial w}{\partial z}\right)+F_z\left(x,y,z,t\right) \tag{3}$$

In the above equations, the C_{ij} are the 9 stiffness coefficients which define an orthorhombic medium (Schoenberg and Helbig 1997). The related quantities $A_{ij}=C_{ij}/\rho$ have the dimensions of velocity squared. The volume density is ρ and $\mathbf{F}\left(x,y,z,t\right)=\left(F_x,F_y,F_z\right)$ is some source term.

The (stress free) boundary conditions at the free surface are specified by

$$\tau_{zz}\big|_{z=0}=C_{13}\frac{\partial u}{\partial x}+C_{23}\frac{\partial v}{\partial y}+C_{33}\frac{\partial w}{\partial z}=0 \tag{4}$$

$$\tau_{xz}\big|_{z=0}=C_{55}\left(\frac{\partial w}{\partial x}+\frac{\partial u}{\partial z}\right)=0 \tag{5}$$

$$\tau_{yz}\big|_{z=0}=C_{44}\left(\frac{\partial v}{\partial z}+\frac{\partial w}{\partial y}\right)=0 \tag{6}$$

and the problem is solved with zero initial data:

$$u\big|_{t=0}=\left.\frac{\partial u}{\partial t}\right|_{t=0}=v\big|_{t=0}=\left.\frac{\partial v}{\partial t}\right|_{t=0}=w\big|_{t=0}=\left.\frac{\partial w}{\partial t}\right|_{t=0}=0 \tag{7}$$

As previously mentioned, the medium has been chosen such that it is composed of plane parallel layers where the elastic parameters, stiffnesses and density $\left(C_{ij}\text{ and }\rho\right)$, do not vary in the horizontal directions but as previously mentioned may vary in an arbitrary manner with depth $\left(z\right)$. As a consequence the $\left(x\text{ and }y\right)$ coordinates may be temporarily removed using finite Fourier transforms. The two dimensional finite Fourier transforms and inverses for the three components of displacement are defined as (Sneddon, 1995)

$$S\left(z,n,m,t\right)=\int_0^a dx\int_0^b dy\,u\left(z,x,y,t\right)\cos\left(\frac{m\pi y}{b}\right)\sin\left(\frac{n\pi x}{a}\right) \tag{8}$$

$$u\left(z,x,y,t\right)=\frac{4}{ab}\sum_{n=0}^{\infty}\sum_{m=0}^{\infty}S\left(z,n,m,t\right)\cos\left(\frac{m\pi y}{b}\right)\sin\left(\frac{n\pi x}{a}\right) \tag{9}$$

$$H(z,n,m,t)=\int_0^a dx\int_0^b dy\, v(z,x,y,t)\sin\left(\frac{m\pi y}{b}\right)\cos\left(\frac{n\pi x}{a}\right) \tag{10}$$

$$v(z,x,y,t)=\frac{4}{ab}\sum_{n=0}^{\infty}\sum_{m=0}^{\infty}H(z,n,m,t)\sin\left(\frac{m\pi y}{b}\right)\cos\left(\frac{n\pi x}{a}\right) \tag{11}$$

$$R(z,n,m,t)=\int_0^a dx\int_0^b dy\, w(z,x,y,t)\cos\left(\frac{m\pi y}{b}\right)\cos\left(\frac{n\pi x}{a}\right) \tag{12}$$

$$w(z,x,y,t)=\frac{4}{ab}\sum_{n=0}^{\infty}\sum_{m=0}^{\infty}R(z,n,m,t)\cos\left(\frac{m\pi y}{b}\right)\cos\left(\frac{n\pi x}{a}\right) \tag{13}$$

After applying the finite forward transforms given above to equations (1) – (3) the following result

$$\begin{aligned}\rho\frac{\partial^2 S}{\partial t^2}=&-k_x^2C_{11}S-k_xC_{13}\frac{\partial R}{\partial z}-k_y^2C_{66}S-k_xk_y\left(C_{12}+C_{66}\right)H+\\&\frac{\partial}{\partial z}\left(C_{55}\frac{\partial S}{\partial z}\right)-k_x\frac{\partial}{\partial z}\left(C_{55}R\right)+F_x\left(k_x,k_y,z,t\right)\end{aligned} \tag{14}$$

$$\begin{aligned}\rho\frac{\partial^2 H}{\partial t^2}=&\left(-k_xk_yC_{66}S-k_x^2C_{66}H\right)-k_xk_yC_{12}S-k_y^2C_{22}H-k_yC_{23}\frac{\partial R}{\partial z}+\\&\frac{\partial}{\partial z}\left(C_{44}\frac{\partial H}{\partial z}\right)-k_y\frac{\partial}{\partial z}\left(C_{44}R\right)+F_y\left(k_x,k_y,z,t\right)\end{aligned} \tag{15}$$

$$\begin{aligned}\rho\frac{\partial^2 R}{\partial t^2}=&k_xC_{55}\frac{\partial S}{\partial z}+k_yC_{44}\frac{\partial H}{\partial z}-\left(k_y^2C_{44}+k_x^2C_{55}\right)R+\\&k_x\frac{\partial}{\partial z}\left(C_{13}S\right)+k_y\frac{\partial}{\partial z}\left(C_{23}H\right)+\frac{\partial}{\partial z}\left(C_{33}\frac{\partial R}{\partial z}\right)+F_z\left(k_x,k_y,z,t\right)\end{aligned} \tag{16}$$

where it is to be remembered that it has been assumed that the stiffnesses do not depend on the horizontal $(x \text{ and } y)$ coordinates. It will initially be assumed that the pseudo – boundaries introduced at $(x=a,\ y=b)$ are perfectly reflecting.

The transformed boundary conditions at the free surface are:

1. Normal Stress:

$$\tau_{zz}\big|_{z=0}=k_xC_{13}S+k_yC_{23}H+C_{33}\frac{\partial R}{\partial z}=0 \tag{17}$$

2. Shear Stress, τ_{xz}:

$$\tau_{xz}\big|_{z=0} = C_{55}\left(\frac{\partial S}{\partial z} - k_x R(z,n,m,t)\right) = 0 \tag{18}$$

3. Shear Stress, τ_{yz}:

$$\tau_{yz}\big|_{z=0} = C_{44}\left(\frac{\partial H}{\partial z} - k_y R\right) = 0 \tag{19}$$

The grid spacing in depth is Δz. The problem is solved with zero initial data so that

$$S\big|_{t=0} = \left.\frac{\partial S}{\partial t}\right|_{t=0} = H\big|_{t=0} = \left.\frac{\partial H}{\partial t}\right|_{t=0} = R\big|_{t=0} = \left.\frac{\partial R}{\partial t}\right|_{t=0} = 0 \tag{20}$$

It will be assumed that at the first 3 grid points at the free surface the $A_{ij} = C_{ij}/\rho$ and volume density (ρ) are independent of the z spatial coordinate. Thus equations (14) – (16) may be written in this region as

$$\frac{\partial^2 S}{\partial t^2} = -k_x k_y \left(A_{12} + A_{66}\right) H - \left(k_y^2 A_{11} + k_y^2 A_{66}\right) S - k_x \left(A_{13} + A_{55}\right) \frac{\partial R}{\partial z} + A_{55} \frac{\partial^2 S}{\partial z^2} \tag{21}$$

$$\frac{\partial^2 H}{\partial t^2} = -k_x k_y \left(A_{12} + A_{66}\right) S - \left(k_y^2 A_{22} + k_x^2 A_{66}\right) H - k_y \left(A_{23} + A_{44}\right) \frac{\partial R}{\partial z} + A_{44} \frac{\partial^2 H}{\partial z^2} \tag{22}$$

$$\frac{\partial^2 R}{\partial t^2} = k_x \left(A_{13} + A_{55}\right) \frac{\partial S}{\partial z} + k_y \left(A_{23} + A_{44}\right) \frac{\partial H}{\partial z} - \left(k_x^2 A_{55} + k_y^2 A_{44}\right) R + + A_{33} \frac{\partial^2 R}{\partial z^2} \tag{23}$$

Employing equations (19), (22) and (25) the finite difference analogues of the above equations have the form, with Δz the spatial depth step and Δt the time step,

At an interior point, where the stiffnesses and density may depend on the spatial coordinate z the finite difference analogues have a more complex form These may be found in an earlier report on this topic. The source term has not been included, however, once a source type has been decided upon the vector components of it may be added.

ABSORBING BOUNDARY AT MODEL BOTTOM

Paraxial approximations for the elastic wave equation analogous to those of the scalar wave equation can also be found. We cannot, however, perform the analysis by considering expansions of the dispersion relation because the differential equations for vector fields are not uniquely specified from their dispersion relations. Instead, we use the scalar case to provide a hint as to the general form of the paraxial approximation and fit the coefficients by matching to the full elastic wave equation. Or as a reasonable alternative, use the 3 scalar wave equations that result from requiring that all *off* terms in the 3 vector coupled wave equations are set equal to zero. These three resulting scalar equations may be written as

$$\frac{\partial^2 S}{\partial t^2} = -\left(k_x^2 A_{11} + k_y^2 A_{66}\right) S + A_{55} \frac{\partial^2 S}{\partial z^2} \tag{24}$$

$$\frac{\partial^2 H}{\partial t^2} = -\left(k_y^2 A_{22} + k_x^2 A_{66}\right) H + A_{44} \frac{\partial^2 H}{\partial z^2} \tag{25}$$

$$\frac{\partial^2 R}{\partial t^2} = -\left(k_y^2 A_{44} + k_x^2 A_{55}\right) R + A_{33} \frac{\partial^2 R}{\partial z^2} \tag{26}$$

Assume a plane wave solution of the form:

$$Q = \exp\left(-i\omega t + ik_z z\right) \quad \left(Q = S, H, R\right). \tag{27}$$

The pseudo-differential operators required will be defined as

$$\left(-i\omega\right) \rightarrow \frac{\partial}{\partial t} \qquad \text{and} \qquad \left(ik_z\right) \rightarrow \frac{\partial}{\partial z}. \tag{28}$$

Consider equation (24) as an example and introduce the plane wave solution, equation (27) to obtain

$$\left(-i\omega\right)^2 S = -k_x^2 A_{11} S - k_y^2 A_{66} S + A_{55} \left(ik_z\right)^2 S. \tag{29}$$

Under the assumption that $S \neq 0$, the requirement that

$$\frac{\left(ik_z\right)^2}{\left(-i\omega\right)^2} = \frac{1}{A_{55}} \left(1 + \frac{k_x^2 A_{11}}{\left(-i\omega\right)^2} + \frac{k_y^2 A_{66}}{\left(-i\omega\right)^2} \right) \tag{30}$$

must be valid, so that a paraxial approximation to the scalar type wave equation has the form

$$\frac{(ik_z)}{(-i\omega)} = \pm\frac{1}{\sqrt{A_{55}}}\left(1+\frac{k_x^2 A_{11}}{(-i\omega)^2}+\frac{k_y^2 A_{66}}{(-i\omega)^2}\right)^{1/2}. \qquad (31)$$

where the "$\pm$" refer to down going and up going waves, respectively. If the combined absolute values of the non-unity parts of the radicals on the RHS of equation (31) can be shown to be much less than one, the following paraxial approximation is obtained

$$\frac{(ik_z)}{(-i\omega)} \approx \pm\frac{1}{\sqrt{A_{55}}}\left(1+\frac{k_x^2 A_{11}}{2(-i\omega)^2}+\frac{k_y^2 A_{66}}{2(-i\omega)^2}\right). \qquad (32)$$

From this equation it follows that

$$(ik_z)(-i\omega) \approx \pm\left(\frac{1}{\sqrt{A_{55}}}(-i\omega)^2+\frac{k_x^2 A_{11}}{2\sqrt{A_{55}}}+\frac{k_y^2 A_{66}}{2\sqrt{A_{55}}}\right). \qquad (33)$$

Reintroducing the pseudo-differential operators leads to

$$\frac{\partial^2 S}{\partial z\partial t}+\frac{1}{\sqrt{A_{55}}}\frac{\partial^2 S}{\partial t^2}+\frac{k_x^2 A_{11}}{2\sqrt{A_{55}}}S+\frac{k_y^2 A_{66}}{2\sqrt{A_{55}}}S=0 \qquad (34)$$

In a similar manner the parabolic approximations for the scalar type wave equations in H and S may be written as

$$\frac{\partial^2 H}{\partial z\partial t}+\frac{1}{\sqrt{A_{44}}}\frac{\partial^2 H}{\partial t^2}+\frac{k_y^2 A_{22}}{2\sqrt{A_{44}}}H+\frac{k_x^2 A_{66}}{2\sqrt{A_{44}}}H=0 \qquad (35)$$

and

$$\frac{\partial^2 R}{\partial z\partial t}+\frac{1}{\sqrt{A_{33}}}\frac{\partial^2 R}{\partial t^2}+\frac{k_y^2 A_{44}}{2\sqrt{A_{33}}}R+\frac{k_x^2 A_{55}}{2\sqrt{A_{33}}}R=0 \qquad (36)$$

Finite difference analogues for upward propagating waves at $z = z_K$ (model bottom), which requires that the grid point at $z = z_{K-1}$ be included, and are consistent with those presented in Clayton and Engquist (1977) will now be given. In the following equations, the superscripts refer to the time point and the subscripts to the z grid point S_K^n. The superscripts $n+1, n$ and $n-1$ refer to the current time point and the two previous time points $\left((n)\Delta t, (n-1)\Delta t\right)$.

$$\left(1+\left(\frac{\Delta z}{\sqrt{A_{55}}\Delta t}\right)\right)S_K^{n+1} = S_{K-1}^{n+1} + S_K^{n-1} - S_{K-1}^{n-1} +$$
$$\left(\frac{\Delta z}{\sqrt{A_{55}}\Delta t}\right)\left(2S_K^n - S_K^{n-1} - S_{K-1}^{n+1} + 2S_{K-1}^n - S_{K-1}^{n-1}\right) - \left(\frac{\Delta z \Delta t A_{11}}{\sqrt{A_{55}}}\right)\left(S_K^{n-1} + S_{K-1}^{n+1}\right) -$$
$$\left(\frac{\Delta z \Delta t A_{66}}{\sqrt{A_{55}}}\right)\left(S_K^{n-1} + S_{K-1}^{n+1}\right) \tag{37}$$

$$\left(1+\left(\frac{\Delta z}{\sqrt{A_{44}}\Delta t}\right)\right)H_K^{n+1} = H_{K-1}^{n+1} + H_K^{n-1} - H_{K-1}^{n-1} +$$
$$\left(\frac{\Delta z}{\sqrt{A_{44}}\Delta t}\right)\left(2H_K^n - H_K^{n-1} - H_{K-1}^{n+1} + 2H_{K-1}^n - H_{K-1}^{n-1}\right) - \left(\frac{\Delta z \Delta t A_{66}}{\sqrt{A_{44}}}\right)\left(H_K^{n-1} + H_{K-1}^{n+1}\right) - \tag{38}$$
$$\left(\frac{\Delta z \Delta t A_{22}}{\sqrt{A_{44}}}\right)\left(H_K^{n-1} + H_{K-1}^{n+1}\right)$$

$$\left(1+\left(\frac{\Delta z}{\sqrt{A_{33}}\Delta t}\right)\right)R_K^{n+1} = R_{K-1}^{n+1} + R_K^{n-1} - R_{K-1}^{n-1} +$$
$$\left(\frac{\Delta z}{\sqrt{A_{33}}\Delta t}\right)\left(2R_K^n - R_K^{n-1} - R_{K-1}^{n+1} + 2R_{K-1}^n - R_{K-1}^{n-1}\right) - \left(\frac{\Delta z \Delta t A_{55}}{\sqrt{A_{33}}}\right)\left(R_K^{n-1} + R_{K-1}^{n+1}\right) - \tag{39}$$
$$\left(\frac{\Delta z \Delta t A_{22}}{\sqrt{A_{33}}}\right)\left(R_K^{n-1} + R_{K-1}^{n+1}\right)$$

NUMERICAL RESULTS

Before addressing the problem of spurious arrivals at the model bottom, those which may occur from the improper specifications of the perfectly reflecting boundaries in the lateral (x, y) plane should be investigated. These can cause numerical accuracy problems at least as bad as those from the finite depth boundary. The model used for this numerical

experiment is given in Table 1, two layers over a halfspace. The layer thickness of the isotropic surface layer is $0.25km$ and the second, orthorhombic layer, is $0.5km$.The halfspace has the same medium parameters as the surface layer. A vertical point force source is located at the surface, as are the receivers. The receivers are placed in a circle, every 2degrees around the source at an offset of 0.5km.Vertical, inline and crossline (xline) components of displacement are computed. Synthetics are first computed for a case where the two perfectly reflecting boundaries are placed at a lateral distance where it assured that they will introduce unwanted arrivals. The numerical experiment is then repeated with the pseudo boundaries at $(x = b, y = c)$ placed at distances where unwanted reflected arrivals from them should not appear in the synthetics. In both cases, the equations derived in the previous section were implemented, so it is assumed (euphemistically) that spurious reflections from the model bottom are not present in these. The results from this numerical experiment are shown in Figures (1) through (3) for the model defined in Table 1 and earlier in this paragraph.

In the second set of numerical experiments surface source and receivers placed along a line at $30\ \text{degrees}$ with respect to the x axis. The same model as was used in the first modeling experiment and given in Table 1 was used. Fifty receivers were placed at the surface with a spacing of $0.01km$.The perfectly reflecting boundaries in the lateral directions have been placed such that cannot contribute unwanted arrivals. This is enhanced by using only half the normal offset range that should be able to be accommodated by the geometry of this model. The vertical, inline and xline components of particle displacement are shown before and after model boundary corrections in Figures (4) through (6).

DISCUSSION AND CONCLUSIONS

Finite difference analogues, accurate to second order in space and time, for a plane parallel orthorhombic $(3D)$ media in which dependence on the horizontal Cartesian coordinates have been removed by finite Fourier transforms have been presented. For the type of elastic medium discussed here, the simplest source type to incorporate is a vertical point source located the origin of the Cartesian system so that $F(z,x,y,t) = \delta(z) f(t) \mathbf{e}_z$ where $\mathbf{e}_z$ is a unit vector in the z direction and $f(t)$ is the time dependence of the source wavelet. This wavelet is most often assumed to be band limited, as the range of its power spectrum in the frequency domain is linearly related to the number of terms required to approximate the two infinite Fourier series summations. The particle displacement may be recovered by applying inverse series summations, also specified above. Absorbing boundary conditions where introduced at the model bottom and appear to properly correct for spurious reflections when compared to a method of computation that is known to remove these unwanted arrivals. This consists of setting the model bottom so far out of range that reflections from it could not be recorded withinin the time window specified. This approach is computationally intensive and not recommended for use in practice. All computations were carried out on a “vintage” Lenovo laptop with 24G of memory.

ACKNOWLEDGEMENTS

The author wishes to thank the sponsors of CREWES and NSERC (Professor G.F. Margrave, CRDPJ 379744-08) for financial support in undertaking this work.

REFERENCES

Mikhailenko, B.G., 1985, Numerical experiment in seismic investigations, Journal of Geophysics, 58, 101-124.

Clayton, R. and Engquist, B., 1980, Absorbing boundary conditions for wave-equation migration, GEOPHYSICS, 45, 895-904.

Reynolds, A.C., 1978, Boundary conditions for the numerical solution of wave propagation problems, Geophysics, 43, 1099-1110.

Schoenberg, M., and Helbig, K., 1997, Orthorhombic media: Modeling elastic wave behavior in a vertically fractured earth: Geophysics, 62, 1954-1974.

Sneddon, I.A, 1995, Fourier Transforms, Dover Publications, New York.

Layer	A11	A22	A33	A44	A55	A66	A12	A13	A23
1	8.0	8.0	8.0	2.5	2.5	2.5	3.0	3.0	3.0
2	9.9	6.023	7.093	1.964	2.448	2.438	1.926	2.074	2.225
Hspace	8.0	8.0	8.0	2.5	2.5	2.5	3.0	3.0	3.0

Table 1. The model used in the computation of synthetics in this report. The Aij have the dimensions of (velocity)2. The surface layer and halfspace are assumed to be isotropic while the layer between them is orthorhombic.

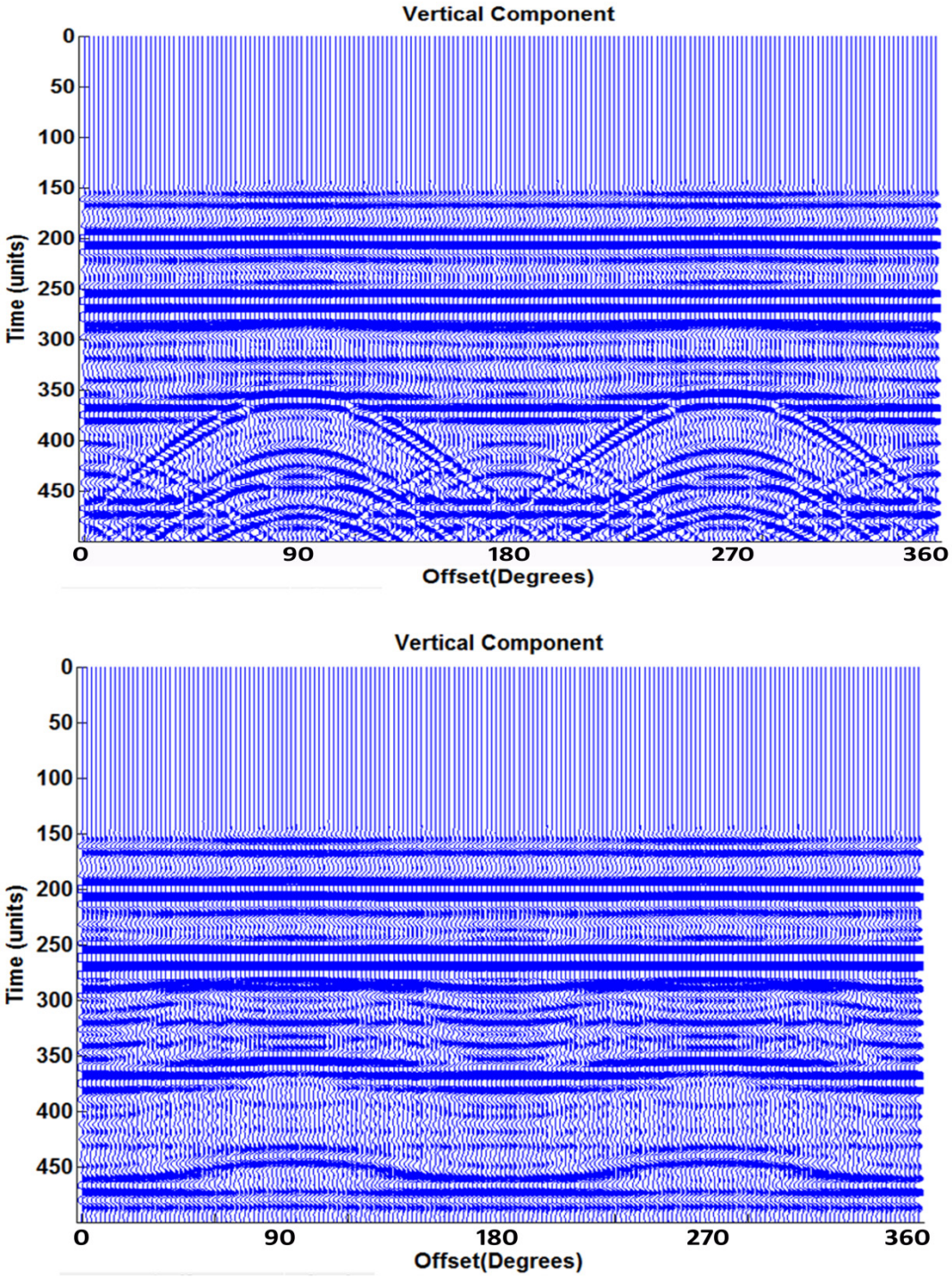

Fig.1. Vertical component of displacement. In the top panel the perfectly reflecting pseudo-boundaries have been placed at distances where they will definitely produce unwanted arrivals during the time length of the synthetic. In the bottom panel these boundaries have been moved to distances where they cannot introduced unwanted reflected arrivals.

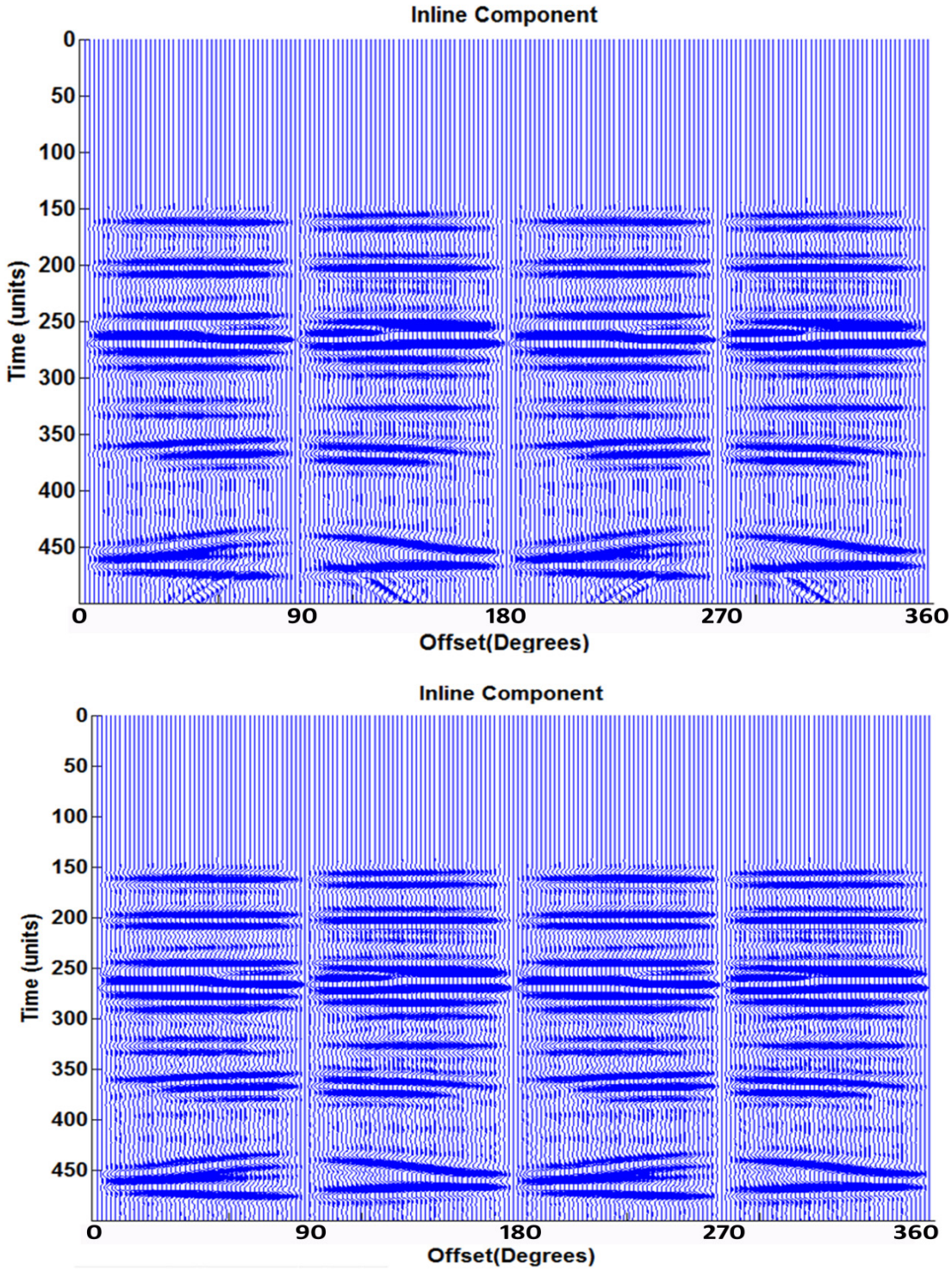

Fig.2. Inline component of displacement. In the top panel the perfectly reflecting pseudo-boundaries have been placed at distances where they will definitely produce unwanted arrivals during the time length of the synthetic. In the bottom panel these boundaries have been moved to distances where they cannot introduced unwanted reflected arrivals.

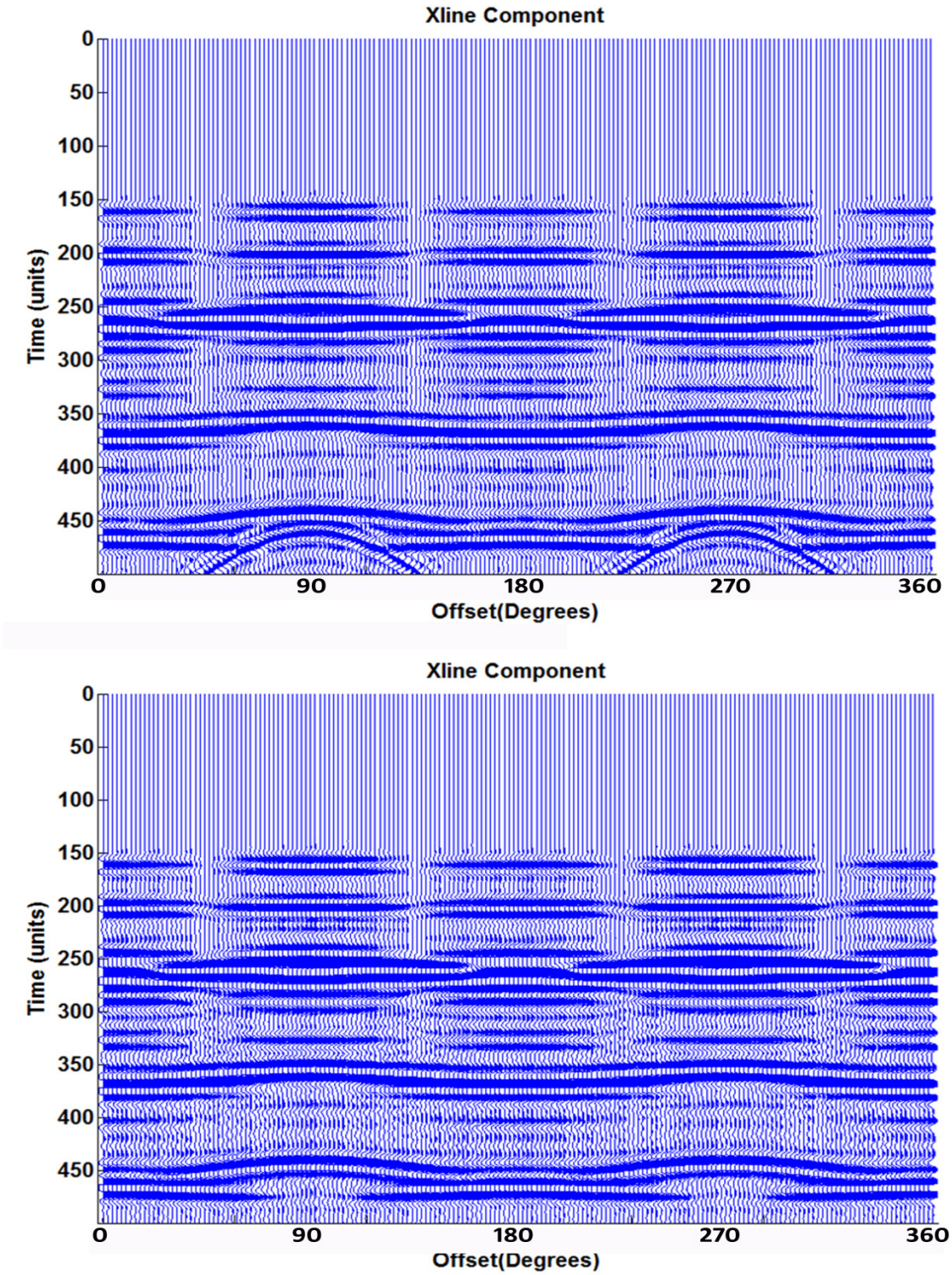

Fig.3. Xline component of displacement. Vertical component of displacement. In the top panel the perfectly reflecting pseudo-boundaries have been placed at distances where they will definitely produce unwanted arrivals during the time length of the synthetic. In the bottom panel these boundaries have been moved to distances where they cannot introduced unwanted reflected arrivals.

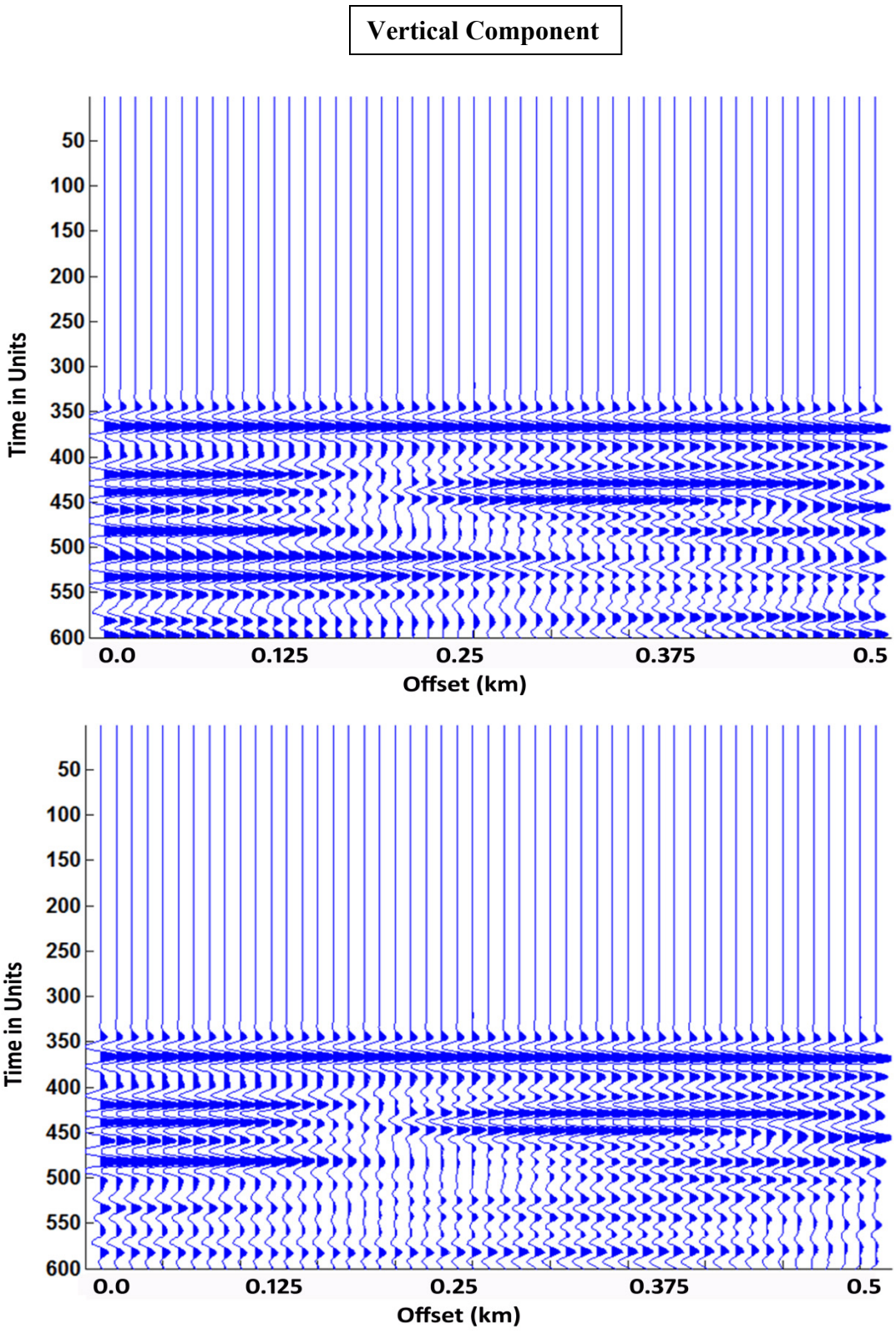

Fig. 4. Vertical component of displacement for the offset case. The top has no corrections made to remove spurious reflected arrivals from the model pseudo – bottom. In the lower panel these corrections have been made using the scalar wave approximations to the three components of particle displacement.

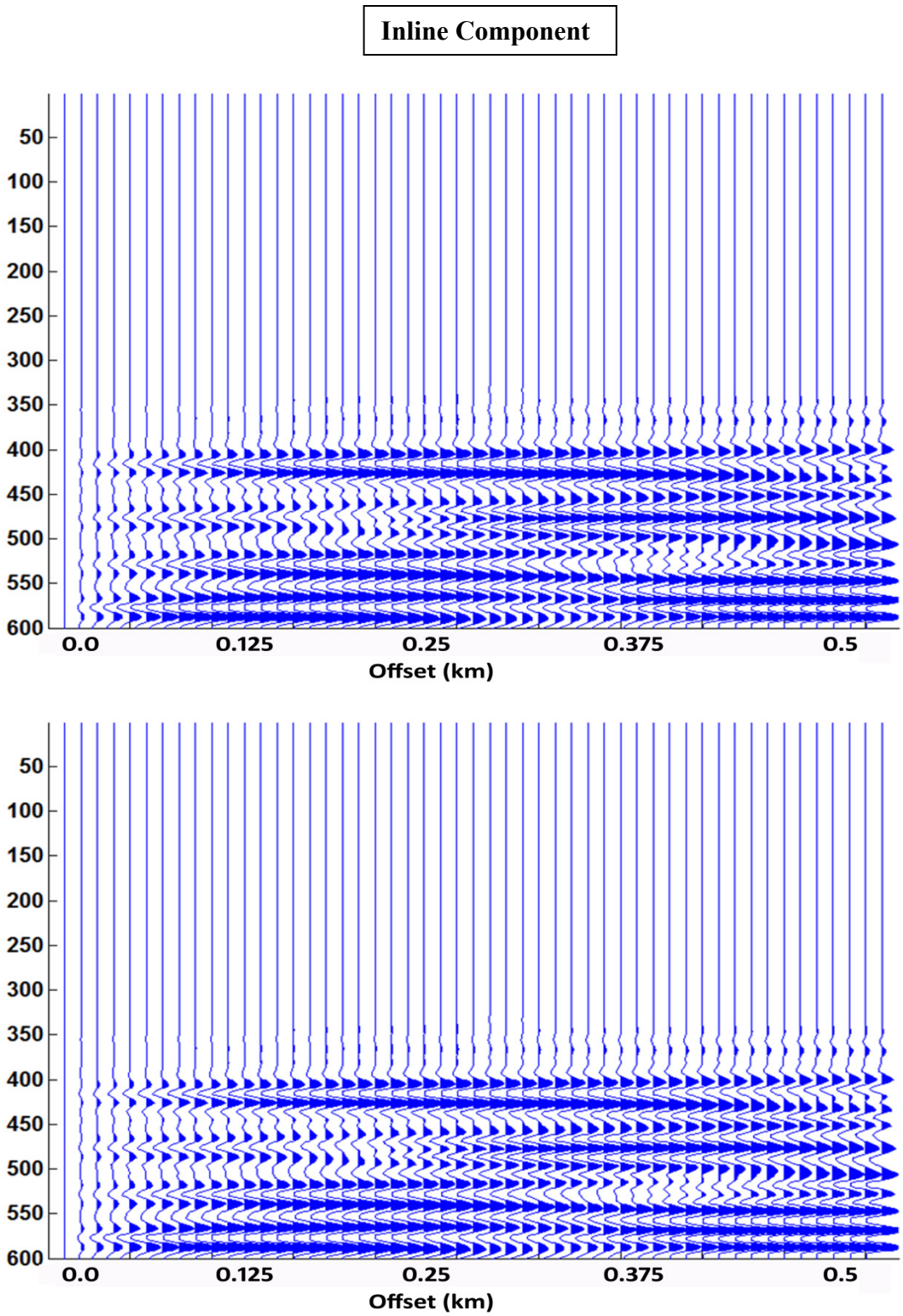

Fig. 5. Inline component of displacement for the offset case. The top has no corrections made to remove spurious reflected arrivals from the model pseudo – bottom. In the lower panel these corrections have been made using the scalar wave approximations to the three components of particle displacement.

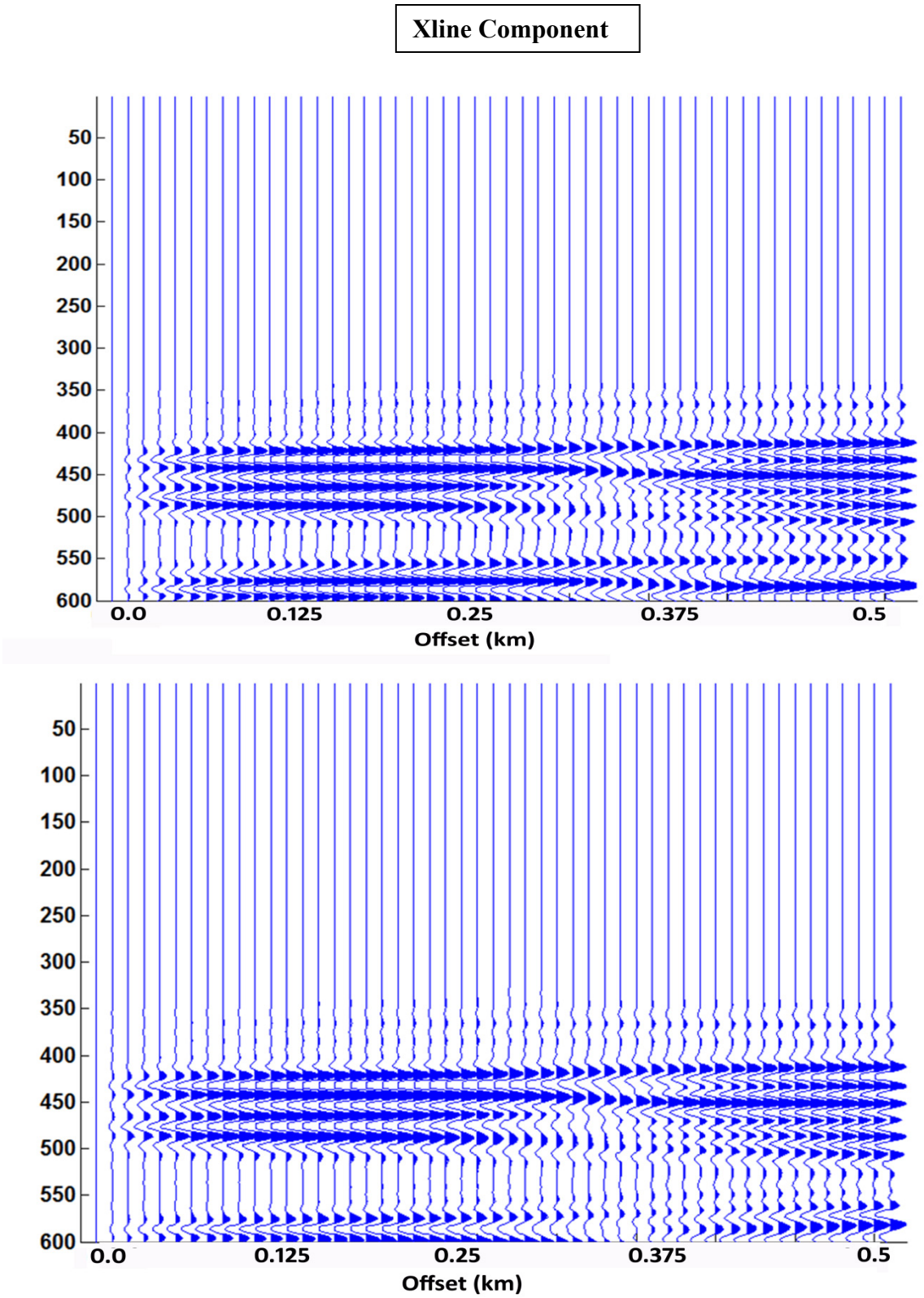

Fig. 6. Xline component of displacement for the offset case. The top has no corrections made to remove spurious reflected arrivals from the model pseudo – bottom. In the lower panel these corrections have been made using the scalar wave approximations to the three components of particle displacement.